Journal of Hydroscience and Hydraulic Engineering
Vol. 13, No. 2, November, 1995, 55 - 67

BEHAVIOR OF DRIFTWOOD AND THE PROCESS OF ITS DAMMING UP

By

Hajime Nakagawa, Kazuya Inoue
Disaster Prevention Research Institute, Kyoto University, Uji City, Kyoto, Japan

Masaaki Ikeguchi
Tunnel Division, Public Works Research Institute, Tsukuba, Ibaraki, Japan

and

Takaki Tsubono
Department of Civil Engineering, Kyoto University, Kyoto, Japan

SYNOPSIS

A numerical simulation model has been developed for computing the behavior of driftwood and of its damming up process when caught between and/or in front of model houses when driftwood debouches into a horizontal two-dimensional flow field. Equations of the rotational motion and the translational motion of driftwood are evaluated dynamically in the Lagrangian form. An interacting combination of Eulerian fluid and Lagrangian driftwood equations were used in which the turbulent diffusivity and the fluctuation component of the rotational angular velocity of the driftwood are given stochastically. The positions and rotational angles of pieces of driftwood, and the time change in the number of pieces caught between and/or in front of the models in the experiments are well explained by the calculations.

INTRODUCTION

During flooding, pieces of driftwood become caught by bridge piers which often results in the destruction of the piers and/or embankment. Destruction of river embankments during flooding produces not only a serious inundation disaster but the destruction of buildings by driftwood caught between and/or in front of them. To clarify the nature of driftwood disasters, we need to understand the mechanism of driftwood behavior and its damming up process. We therefore first have used a Eulerian calculation method to accurately determine the flow field then evaluated the equation of the rotational motion of driftwood dynamically as well as the equation of translational motion in the Lagrangian form. The mathematical model has been checked against experimental results found for driftwood behavior in a horizontal two-dimensional flow field. Lastly, hydraulic model experiments on the damming up process have been made, and the numerical simulation model of this phenomenon has been compared with the experimental data.

BASIC EQUATIONS OF FLUID AND DRIFTWOOD MOTION

Basic Equations of Fluid Motion

The basic equations used to calculate the behavior of an overland flood flow are the horizontal two-dimensional momentum and continuity equations:

$$\frac{\partial M}{\partial t}+\frac{\partial (uM)}{\partial x}+\frac{\partial (vM)}{\partial y}=-gh\frac{\partial H}{\partial x}-\frac{1}{2}fu\sqrt{u^2+v^2}+\nu\left(\frac{\partial}{\partial x}h\frac{\partial u}{\partial x}+\frac{\partial}{\partial y}h\frac{\partial u}{\partial y}\right)$$

$$+\frac{\partial}{\partial x}\left\{h\left(2A_h\frac{\partial u}{\partial x}-\frac{2}{3}k\right)\right\}+\frac{\partial}{\partial y}\left\{hA_h\left(\frac{\partial u}{\partial y}+\frac{\partial v}{\partial x}\right)\right\}+\frac{\tau_{sx}}{\rho} \quad (1)$$

$$\frac{\partial N}{\partial t}+\frac{\partial(uN)}{\partial x}+\frac{\partial(vN)}{\partial y}=-gh\frac{\partial H}{\partial y}-\frac{1}{2}fv\sqrt{u^2+v^2}+\nu\left(\frac{\partial}{\partial x}h\frac{\partial v}{\partial x}+\frac{\partial}{\partial y}h\frac{\partial v}{\partial y}\right)$$
$$+\frac{\partial}{\partial y}\left\{h\left(2A_h\frac{\partial v}{\partial y}-\frac{2}{3}k\right)\right\}+\frac{\partial}{\partial x}\left\{hA_h\left(\frac{\partial v}{\partial x}+\frac{\partial u}{\partial y}\right)\right\}+\frac{\tau_{sy}}{\rho} \quad (2)$$

$$\frac{\partial h}{\partial t}+\frac{\partial M}{\partial x}+\frac{\partial N}{\partial y}=0 \quad (3)$$

where M, N = the water discharge per unit width in x and y directions, i.e., $M = uh$ and $N = vh$; u and v = the respective depth-averaged velocity components in the x and y directions; h = the water depth; H = the water level, i.e., $H = h + z_b$, z_b = the elevation of the bed; ρ = the density of the fluid; g = the acceleration due to gravity; f = the friction coefficient at the bottom; ν = the kinematic viscosity; A_h = the kinematic eddy viscosity horizontally; k = the turbulent energy; τ_{sx} and τ_{sy} = the shear stresses at the water surface in the x and y directions; t = time; and x and y = the coordinate axes taken in the horizontal directions. According to Hosoda and Kimura (1) the horizontal kinematic eddy viscosity, A_h, and turbulent energy, k, are

$$A_h = ahu_* \quad ; \quad k = 2.07u_*^2 \quad (4)$$

where u_* = the friction velocity; and a = a numerical constant with the value 0.3. For the friction coefficient at the bottom, f, alternatively the laminar or turbulent flow resistance formula based on the Reynolds number is used;

$$f = 6/Re \ \ (Re < 400) \quad ; \quad \sqrt{2/f} = 3.0 + 5.75\log Re\sqrt{f/2} \ \ (Re \geq 400) \quad (5)$$

where Re = Reynolds number defined by $Re = \sqrt{u^2+v^2}h/\nu$.

We assume that the shear stresses that the flood flow experiences at the water surface, τ_{sx} and τ_{sy}, are generated as the reaction of the drag force acting on the driftwood;

$$\tau_{sx} = \frac{1}{A}\sum_{k=1}^{N_t}\left\{\frac{1}{2}\rho C_{Dx}W_k(u_k-U_k)A_{kx}\right\} \ ; \ \tau_{sy} = \frac{1}{A}\sum_{k=1}^{N_t}\left\{\frac{1}{2}\rho C_{Dy}W_k(v_k-V_k)A_{ky}\right\} \quad (6)$$

where u_k and v_k = the respective driftwood velocity components in the x and y directions; U_k and V_k = the respective local velocity components of the fluid in the x and y directions at the position of the centroid of the driftwood; $W_k = \sqrt{(u_k-U_k)^2+(v_k-V_k)^2}$; A_{kx} and A_{ky} = the respective projected areas of the submerged part of the driftwood in the x and y directions; and C_{Dx} and C_{Dy} = the respective coefficients of the x and y components of the drag force; A = the area of the water surface, written $A = \Delta x\Delta y$ (Δx and Δy = the grid sizes of the finite difference equations); and N_t = the number of total pieces of driftwood in area A.

Basic Equations of Driftwood Motion

It is assumed that no driftwood coalescence or breakup occurs. This implies that the pieces of driftwood are sufficiently dispersed so that collisions between them are infrequent. The drag forces produced by the velocity difference between the fluid and driftwood and the body force component produced by the gradient of the water surface are considered external forces. On the basis of these assumptions, each piece of driftwood, individually labeled by subscript k, is assumed to obey the following equations

$$\frac{dX_k}{dt} = u_k \quad ; \quad \frac{dY_k}{dt} = v_k \quad (7)$$

$$(m_k + mC_M)\frac{du_k}{dt} = m(1+C_M)\frac{U_k}{dt} - m_k g\frac{\partial H_k}{\partial x} - \frac{1}{2}\rho C_{Dx}W_k(u_k-U_k)A_{kx} \quad (8)$$

$$(m_k + mC_M)\frac{dv_k}{dt} = m(1+C_M)\frac{V_k}{dt} - m_k g\frac{\partial H_k}{\partial y} - \frac{1}{2}\rho C_{Dy} W_k (v_k - V_k) A_{ky} \quad (9)$$

where X_k and Y_k = the position of the centroid of the driftwood; m_k = the mass of the driftwood, i.e., $m_k = \rho_d \pi r^2 \ell$; ρ_d =; the density of the driftwood; π =;the ratio of the circumference of a circle to its diameter; r =;the radius of the driftwood; ℓ =; its length; m = the mass of the fluid occupied by the volume of a piece of driftwood; C_M = the virtual mass coefficient; and H_k = the water level at the position of the centroid of the driftwood. The second terms of the right side of the Eqs.(8) and (9) are the body forces produced by the gradient of the water surface. As the translational motion of the driftwood is supposed to be restricted on the water surface, it will be possible to evaluate the body forces in such a way. We neglect the horizontal component of the buoyancy force term in the horizontal two-dimensional coordinate systems because it acts vertically.

The rotational motion around the axis of the centroid of the driftwood is described by evaluating the moment N_o produced by the hydrodynamic force acting on the driftwood. On the supposition that the driftwood can be divided into two pieces at the centroid, "c", and that the drag force acts on both centroids, "a" and "b", of these pieces (Fig.1), the rotational motion of the driftwood is written as

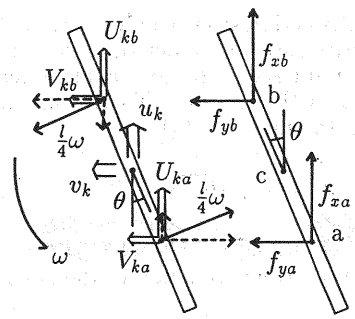

Fig.1 Definition sketch of the rotational angle of pieces of driftwood

$$Id^2\theta_k/dt^2 = \sum N_0 = (\ell/4)\{(f_{xa} - f_{xb})\sin\theta_k - (f_{ya} - f_{yb})\cos\theta_k\} \quad (10)$$

where

$$f_{xa} = (1/2)\rho C_{Dx}\sqrt{(U_{ka} - u_k - u_{rka})^2 + (V_{ka} - v_k - v_{rka})^2}(U_{ka} - u_k - u_{rka})(A_{kx}/2) \quad (11)$$

$$f_{ya} = (1/2)\rho C_{Dy}\sqrt{(U_{ka} - u_k - u_{rka})^2 + (V_{ka} - v_k - v_{rka})^2}(V_{ka} - v_k - v_{rka})(A_{ky}/2) \quad (12)$$

$$f_{xb} = (1/2)\rho C_{Dx}\sqrt{(U_{kb} - u_k - u_{rkb})^2 + (V_{kb} - v_k - v_{rkb})^2}(U_{kb} - u_k - u_{rkb})(A_{kx}/2) \quad (13)$$

$$f_{yb} = (1/2)\rho C_{Dy}\sqrt{(U_{kb} - u_k - u_{rkb})^2 + (V_{kb} - v_k - v_{rkb})^2}(V_{kb} - v_k - v_{rkb})(A_{ky}/2) \quad (14)$$

$$u_{rka} = (\ell/4)(d\theta_k/dt)\sin\theta_k \ , \quad v_{rka} = -(\ell/4)(d\theta_k/dt)\cos\theta_k \quad (15)$$

$$u_{rkb} = -(\ell/4)(d\theta_k/dt)\sin\theta_k \ , \quad v_{rkb} = (\ell/4)(d\theta_k/dt)\cos\theta_k \quad (16)$$

θ_k = the rotational angle of the piece of driftwood; I = the moment of inertia around the centroid,"c", which is written as $I = m_k(r^2/4 + \ell^2/12)$. The rotational motion of the driftwood is also supposed to be restricted on the water surface and the rotation on the vertical plane is not considered. The rotational angle of the piece of driftwood can be evaluated deterministically from these equations, but the results of a statistical analysis of the experiments are also considered (described later).

As the motion of the piece of driftwood is restricted near the water surface, the depth averaged velocity components of the fluid, U_k and V_k, must be transformed into the surface velocity components. For example, for $Re > 400$, the following relations are used

$$U_k \to \frac{5.5 + 5.75\log(u_* h/\nu)}{3.0 + 5.75\log(u_* h/\nu)}U_k \ ; \ V_k \to \frac{5.5 + 5.75\log(u_* h/\nu)}{3.0 + 5.75\log(u_* h/\nu)}V_k \quad (17)$$

As it is very difficult to solve these equations analytically, numerical calculations are made by approximating the equations to finite difference equations. In the previous study (2), we calculated fluid flow behavior using the first order up-wind finite difference equations that had been developed for the calculation of overland flood flows (3). The calculated results by using this

numerical simulation method did not show good agreement with the experimental ones because the numerical viscosity (artificial viscosity) in the calculations weakened the water flow velocity, resulting in slower calculated movement of the driftwood than found experimentally. Therefore we here have introduced the Adams–Bashforth scheme in the time integration, and the QUICK scheme in the integration of the convection term in the momentum equations. For the driftwood motion, time–forward and space–centered schemes are adopted, the velocity components of the driftwood being obtained explicitly.

Fluctuation of Driftwood Position

Driftwood position can be evaluated by integrating the equations $dX_k/dt = u_k$ and $dY_k/dt = v_k$, deterministically under suitable initial conditions, but they fluctuate due to disturbances at the water surface. Hence, we introduce the fluctuation components of driftwood position ΔX_k and ΔY_k in the model. These components ΔX_k and ΔY_k are considered to be evaluated by referring to Dukowicz (4)

$$\Delta X_k = \sqrt{4K_x\Delta t}\mathrm{erf}^{-1}(\alpha) \;\; ; \;\; \Delta Y_k = \sqrt{4K_y\Delta t}\mathrm{erf}^{-1}(\beta) \tag{18}$$

where α, β = random variables independently and uniformly distributed in the range [0,1], and erf^{-1} = the inverse function of the error function, erf, given by

$$\left.\begin{aligned} \mathrm{erf}(s) &= \{1 - \Phi(\sqrt{2}s)\} = \frac{1}{\sqrt{\pi}}\int_s^{\infty} \exp(-\eta^2)d\eta \\ \Phi(s) &= \frac{1}{\sqrt{2\pi}}\int_{-\infty}^{s} \exp(-\eta^2/2)d\eta \end{aligned}\right\} \tag{19}$$

As for the diffusion coefficient of the driftwood, the relations $K_x/u_*h = 0.629$ and $K_y/u_*h = 0.208$, are used referring to the previous works (5), (6). Consequently, the driftwood position is estimated by adding the turbulent fluctuation component to the component obtained deterministically from the equations of motion;

$$\left.\begin{aligned} X_k^{n+1} &= X_k^n + u_k^n\Delta t + \sqrt{4K_x\Delta t}\mathrm{erf}^{-1}(\alpha) \\ Y_k^{n+1} &= Y_k^n + v_k^n\Delta t + \sqrt{4K_y\Delta t}\mathrm{erf}^{-1}(\beta) \end{aligned}\right\} \tag{20}$$

Rotational Angle of Driftwood

The rotational angle of a piece of driftwood can be evaluated deterministically by solving Eq.(10), but it must be influenced by fluctuation in the fluid flow. Indeed, even in a uniform flow field, driftwood flows down with rotational motion having the mean angular velocity $\overline{\omega} \simeq 0$ and the standard deviation $\sigma_\omega = 81.6Fr$ (Fr = Froude number defined by $Fr = \sqrt{(u^2+v^2)/gh}$) (5). This suggests that the characteristics of the fluctuation of the rotational angle of the driftwood are expressed by the characteristics of the angular velocity. Accordingly, we consider two cases; the one in which the rotational angle, θ_k, is determined only by the angular velocity, ω_d, obtained deterministically, the other in which it is determined by both ω_d and ω_p. These two cases are shown as

$$d\theta_k/dt = \omega_d \quad ; \quad d\theta_k/dt = \omega_d + \omega_p \tag{21}$$

where ω_d = the angular velocity of the piece of driftwood obtained from Eq.(10) deterministically; and ω_p = the fluctuation of the angular velocity of the driftwood evaluated stochastically.

Assuming that the fluctuating component of the rotational angular velocity of a piece of driftwood follows a normal distribution (5), its distribution function, Φ, is given by

$$\Phi\left(\frac{\omega_p - \overline{\omega}}{\sigma_\omega}\right) = \frac{1}{\sqrt{2\pi}}\int_{-\infty}^{\frac{\omega_p-\overline{\omega}}{\sigma_\omega}} \exp\left(-\frac{\eta^2}{2}\right)d\eta \tag{22}$$

and $\gamma(=(\omega_p - \overline{\omega})/\sigma_\omega)$ is obtained from the inverse function, Φ^{-1}, for uniformly distributed random numbers within [0,1]. After γ is obtained, ω_p is estimated from $\omega_p = \gamma\sigma_\omega + \overline{\omega}$.

DRIFTWOOD BEHAVIOR

Experimental Apparatus and Method

The experimental set-up used to study two-dimensional driftwood behavior is shown in Fig.2. The flood plain area is 170 cm long and 160 cm wide. A wooden channel (20 cm wide, 150 cm long, 20 cm deep) set up at one side of the flood plain models the breach point of a levee. The bed slope of the flood plain is zero and that of the channel 1/500. The flood plain is enclosed by high banks which prohibit drainage of flood water from the area, except at the opening (20 cm wide) for the outflow of water and driftwood at the downstream end. First the steady state flow was produced on the flood plain by supplying water at constant discharge at the upstream end of the channel. Then driftwood was introduced using a driftwood feeder, 94 cm long, which supplies 72 pieces of driftwood instantaneously to the channel. In the experiments, cylindrical pieces of driftwood 2.5 cm long with a diameter of 2.2 mm and a mass density of 0.83 g/cm^3 were used. The scattering process was recorded by video camera, and the recorded image data was used to analyze the positions and rotational angles of the pieces. A constant water supply with a discharge of 500 cm^3/sec was maintained. Because the process of driftwood scattering may be influenced by fluctuations of the water flow velocity at the surface, the experiments were repeated 4 times under the same hydraulic conditions.

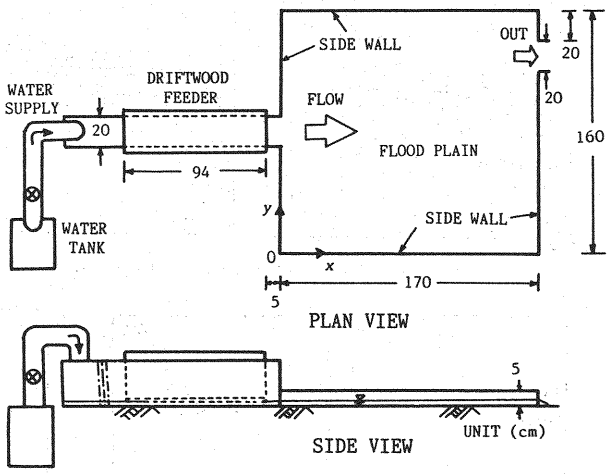

Fig.2 Experimental set-up for measuring the two-dimensional flow behavior of driftwood

Initial and Inflow Conditions for the Calculations

The grid sizes used in the calculation are $\Delta x = \Delta y = 5$ cm, $\Delta t = 0.008$ sec. The characteristics of the driftwood, its density and length, are set at the same ones as in the experiments. The drag coefficients of the driftwood, C_{Dx} and C_{Dy}, used in the calculations are both 1.0, and the virtual mass coefficient, C_M, is 1.0. The initial conditions of the flow field were obtained by solving Eqs.(1), (2), and (3) under the conditions of a constant water discharge (500 cm^3/sec) and no driftwood inflow. After the steady state flow field was reached, the inflow parameters of the driftwood (position, rotational angle, and inflow timing) obtained by analysis of the video images, were given at the breach point ($x = 0$ cm).

Comparison of the Experimental and Calculated Results

Fig.3 shows a comparison of the experimental and calculated surface velocity vectors of the fluid before driftwood debouches into the field. Fig.3(a) shows the experimental vectors, Fig.3(b) the vectors calculated by the proposed method, and Fig.3(c) the vectors calculated obtained using a previous method (the first order up-wind finite difference scheme). From these figures, we see that the calculated results obtained using the proposed method (Fig.3[b]) are in very good agreement with the experimental ones. The agreement of the flow patterns near the exit at the downstream end are particularly good, and this coincidence markedly improves the calculated behavior of the driftwood (Fig.6). Fig.4 shows driftwood behavior calculated under the conditions that the initial angle of the driftwood to the water flow at the inflow boundary is zero and the fluctuation component of the angular velocity, ω_p, also is zero in RUN C. The driftwood moves parallel to the direction of the main flow of the fluid. Fig.5 shows driftwood behavior calculated under the conditions that the initial angle of the driftwood to the water flow

at the inflow boundary is 90° and $\omega_p = 0$ in RUN C. The number of pieces of driftwood whose longer axes are along the direction of the main flow of the fluid appears to increase with time. As very reasonable calculated results were obtained as shown in these figures, the numerical simulation method seems to be valid.

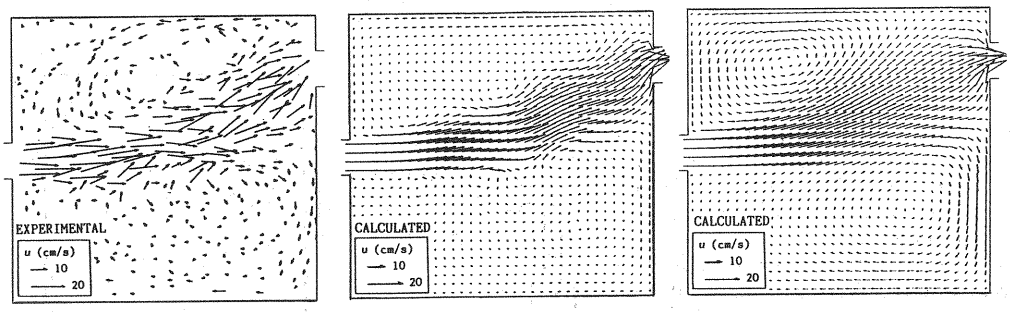

Fig.3 Comparison of the experimental and calculated flow patterns

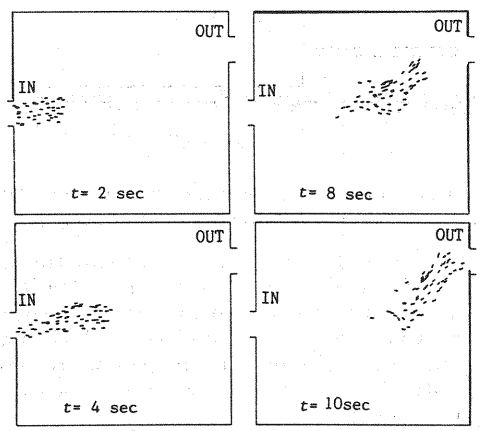

Fig.4 Calculated positions and rotational angles of the driftwood ($\theta_0 = 0°$)

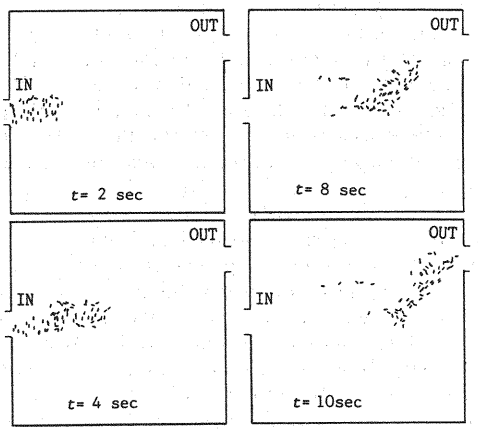

Fig.5 Calculated positions and rotational angles of the driftwood ($\theta_0 = 90°$)

Fig.6 shows comparisons of the experimental and calculated results of positions and rotational angles of the pieces of driftwood in the case of RUN C. The left column gives the results of calculation with $d\theta_k/dt = \omega_d$, the right column those with $d\theta_k/dt = \omega_d + \omega_p$, and the center column the experimental results. The calculated results for $d\theta_k/dt = \omega_d + \omega_p$ show very good agreement with the experimental ones, especially at $t = 20$ sec.

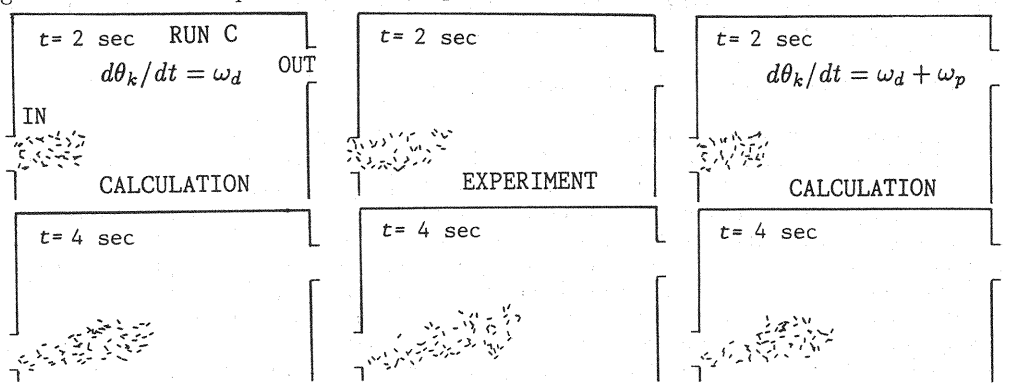

Fig.6 Comparisons of the experimental and calculated positions and rotational angles of the driftwood

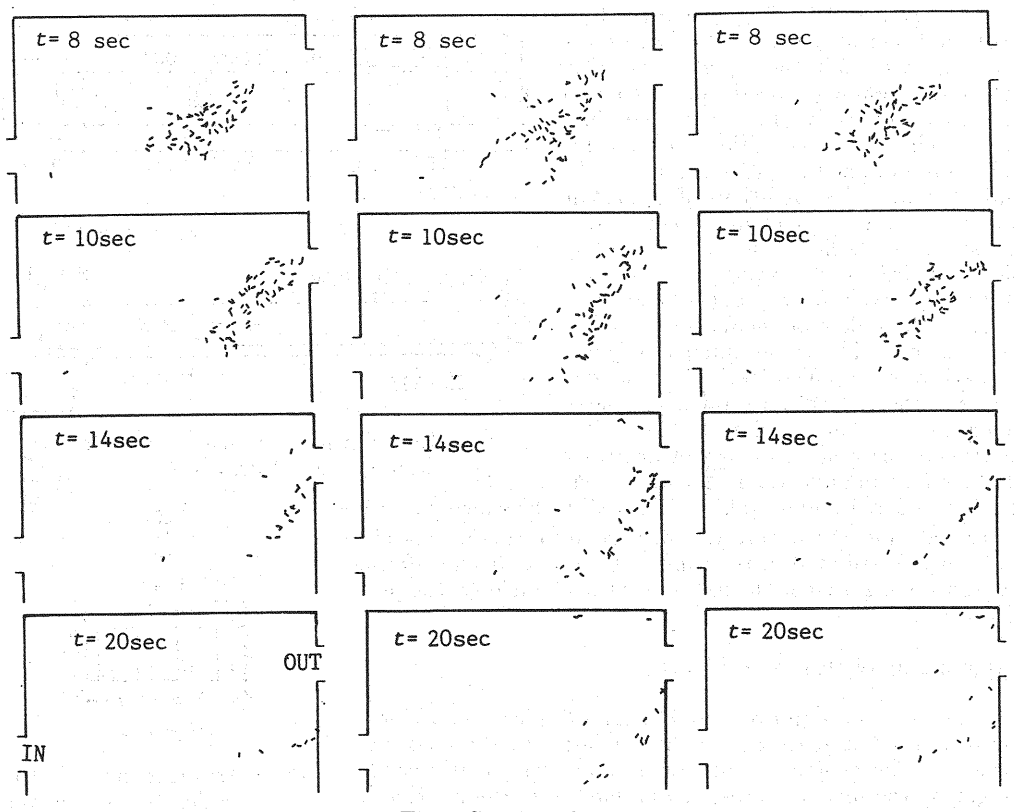

Fig.6 Continued

THE DRIFTWOOD DAMMING UP PROCESS

Hydraulic model experiments on the damming up process caused by driftwood caught between and /or in front of buildings were carried out. The numerical simulation model of this phenomenon was compared with experimental results.

Experimental Apparatus and Method (7)

An experimental flume 30 cm wide, 30 cm deep, and 900 cm long, with a slope of 1/500 was used (Fig.7). Some model structures (hereafter called "model houses") were set in the flow about 6.2 m from the upstream end of the channel. These model houses (5 cm wide, 10 cm long, and 10 cm high) were arranged as shown in Fig.8. The clearance between them was set at 2.5 cm. After the designated water discharge was supplied and the steady state was obtained, pieces of driftwood were supplied by the driftwood feeder, a type of conveyor belt, located about 1.5 m from the upstream end of the channel. The number of pieces of driftwood supplied by the feeder per unit width and time ($= C_{sp}$) varies with the rotational velocity of the pulley of the conveyor belt. Ten pieces of driftwood were lined up twenty-nine deep transversely on the belt (total pieces 290). In these model experiments, 3.0, 4.0, 5.0, 6.0, and 7.0 cm long, cylindrical pieces of driftwood with a diameter of 2.2 mm and a mass density of 0.83 g/cm^3 were used. Water discharge was set at Q =0.5, 1.0, and 1.5 ℓ/sec. The inflow rate of driftwood per unit width and time, C_{sp}, was set at 0.40, 0.68, and 1.93 pieces/sec/cm. Thus experiments were made for 45 hydraulic conditions.

Initial and Inflow Conditions in the Calculations

The grid sizes of calculation were $\Delta x = 5$ cm longitudinally, $\Delta y = 1.25$ cm transversely, and

$\Delta t = 0.004$ sec. The characteristics of the driftwood, density, length, etc. were set at the same ones as in the experiments. The calculation domain ranged from the site of driftwood supply to the end of the channel. The initial conditions of the flow field were obtained by solving Eqs.(1), (2), and (3) under the conditions of a constant water discharge without driftwood. After the steady state flow field was reached, 29 pieces of driftwood, arranged transversely at 1 cm intervals were supplied simultaneously at the inflow boundary with a velocity of zero. The same number of pieces similarly were supplied 10 times at the designated time intervals, a total of 290 pieces being used in each experiment. The initial rotational angle of the pieces of driftwood at the inflow boundary was not measured. Random variables uniformly distributed in the range [0,1] were generated, and these were transformed into random variables uniformly distributed in the range -90°～ 90°, the transformed variables being used as the initial rotational angles of the pieces of driftwood.

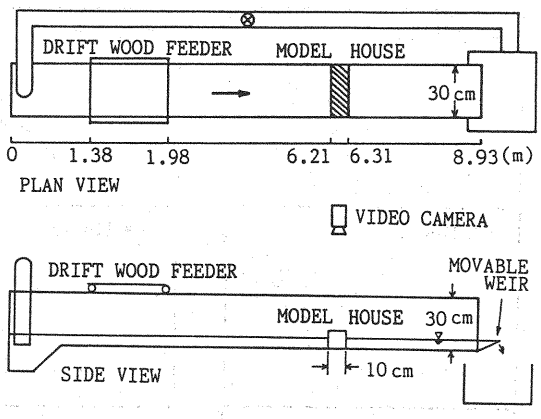

Fig.7 Experimental flume used for the damming up of driftwood

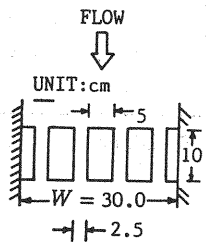

Fig.8 Arrangement of the model houses in the flume

Damming up of Driftwood Model

The positions and rotational angles of pieces of driftwood can be evaluated by the numerical simulation method described earlier. The geometric conditions under which driftwood is caught by the model houses are obtained from the relation between the positions and rotational angles of the pieces of driftwood and the positions of the houses. The relationship between the positions of five pieces of driftwood and two model houses is shown in Fig.9. Three cases are considered as conditions under which driftwood is caught by the model houses: 1) A number (2) of pieces of driftwood (Fig.9) will be caught between houses due to the geometric conditions; 2) When a piece of driftwood with a large rotational angle, such as number (4) in Fig.9, approaches a model house and the position of its centroid is located near the center of the front face of the model house, as at location "b" or "c", and the driftwood will be stopped in front of a model house with its longer axis parallel to the front face of the house. At that time, on the basis of the experimental results, we consider the rotational angle of the driftwood to be in the range of $80° \leq \theta_k \leq 90°$. 3) The piece of driftwood numbered (1), (3), or (5) will be caught once other pieces have been caught between the houses. In this case, the probability of a piece of driftwood being caught depends on the amount of driftwood already piled up between houses. This probability can be assessed in hydraulic experiments.

Fig.10 shows the relationship between the number of pieces of driftwood, n, caught between houses, and the probability, $p(n)$, that driftwood coming from the rear also will be caught by the n pieces of driftwood already stopped. The experimental data are very scattered, but the fitted curve of the mean values gives

$$p(n) = 0.098n^2 \qquad (23)$$

To determine which pieces of driftwood will be caught, the random variable, q, uniformly distributed in the range [0,1], is generated for each piece of driftwood flowing down the channel.

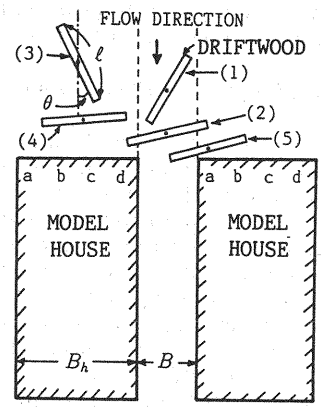

Fig.9 Relation between driftwood position, the rotational angle, and the positions of the model houses used to dam up the driftwood

When the condition, $p(n) > q$, is satisfied the driftwood is considered to be caught. If $n > 3$, $p(n) = 1.0$ and all pieces of driftwood coming from the rear are considered to be caught.

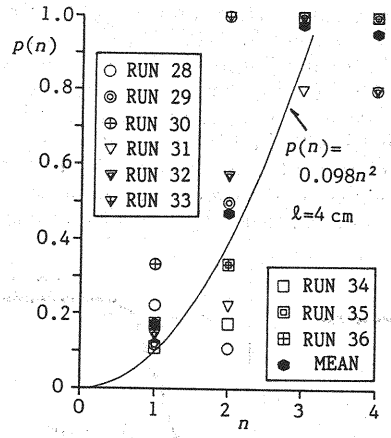

Fig.10 Relation between the number of pieces of driftwood caught between the houses, n, and the probability, $p(n)$, that driftwood arriving from the rear will be caught by the n pieces of driftwood

Comparison of the Experimental and Calculated Results

A comparison of the experimental and calculated temporal changes in the halting rate, $\alpha(t)$, of the driftwood is shown in Fig.11 for RUNS 28, 29, and 30, the halting rate, $\alpha(t)$, being the ratio of the number of pieces of driftwood caught between or at the front faces of the houses to the total amount of driftwood (290 pieces) supplied at the inflow boundary. Here $t = 0$ sec is the time at which the first of the 290 pieces of driftwood supplied at the upstream in the flume arrives at the model house. The experimental conditions for each RUN are given in the figure.

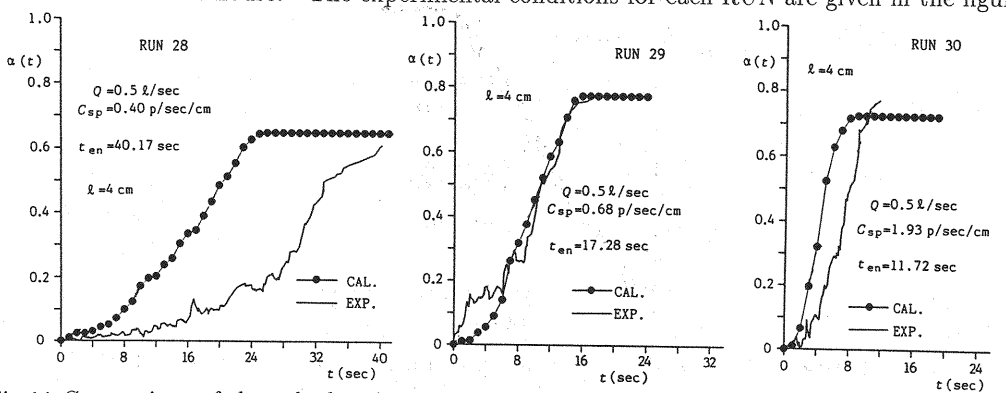

Fig.11 Comparison of the calculated and the experimental halting rate (RUNs 28, 29, and 30)

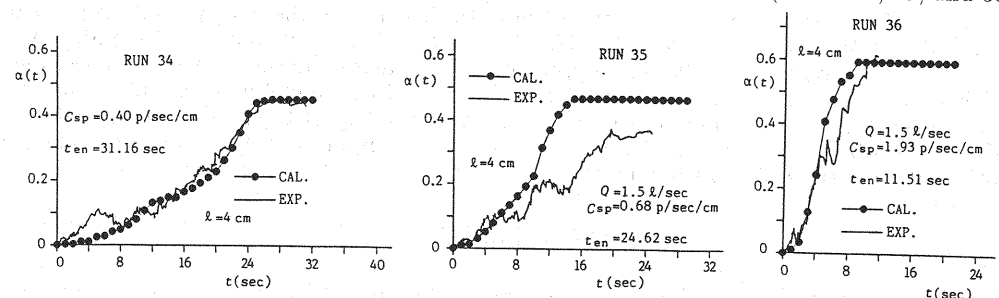

Fig.12 Comparison of the calculated and the experimental halting rate (RUNs 34, 35, and 36)

Fig.12 shows the same comparisons for RUNS 34, 35, and 36, and Fig.13 those for RUNS 52, 53, and 54. The length of each piece of driftwood, ℓ, is 6 cm in these RUNs. The experimental findings for both the final halting rate, $\alpha(t_{en})$, and the time variations of that rate, $\alpha(t)$, are well explained by the calculations, except for RUN 28 where t_{en} is the value of t when the last piece of driftwood arrives at the model house. Although the water discharge in RUN 28 is 500 cc/sec and t_{en}=40.17 sec, the value of t_{en} in the other RUNs with same water discharge was about 30 sec. As only RUN 28 has a large t_{en} value, it may not be suitable for the experimental results. The reason why t_{en} in RUN 28 had the large value of t_{en} = 40.17 sec is not clear, but it may be the result of problems in driftwood supply. Note that the experimental results for RUN 46, in which the length of a piece of driftwood is 6 cm but the other experimental conditions are the same as in RUN 28, are well explained by the calculations (Fig.14).

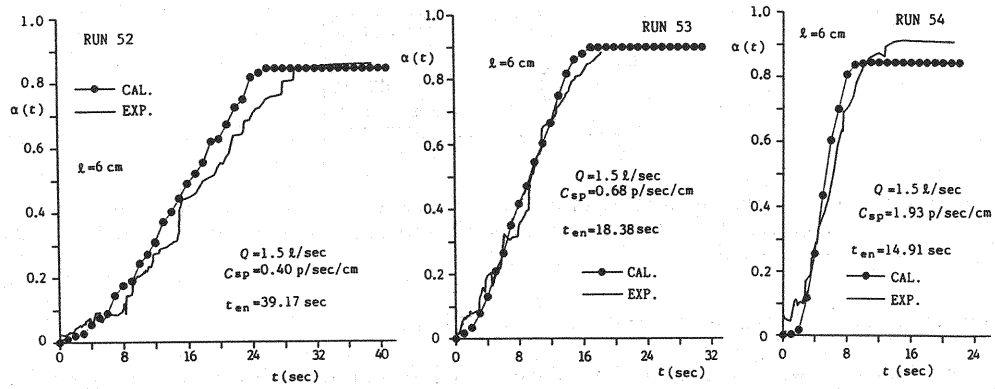

Fig.13 Comparison of the calculated and the experimental halting rate (RUNs 52, 53, and 54)

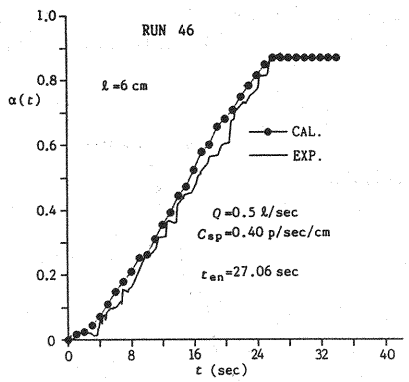

Fig.14 Comparison of the calculated and the experimental halting rate, $\alpha(t)$ (RUN 46).

Fig.15 shows comparisons between the experimental and calculated water surface profiles before and after pieces of driftwood were caught at the houses. In these figures, all the driftwood has arrived at the model houses at t = 90 sec. At t = 0, no driftwood has arrived, but the water level has already risen due to the presence of the model houses. At t = 90 sec, pieces of driftwood have been caught between and/or in front of the model houses, and the dammed up water level has risen markedly because the relative velocity of the fluid as compared to the driftwood has become large. Although the water surface is measured at only two points, the depths obtained are well explained by the calculations.

CONCLUSIONS

The basic equations for fluid and driftwood that were used in the calculations first were refined to increase the accuracy of the calculated results. The finite difference scheme of the

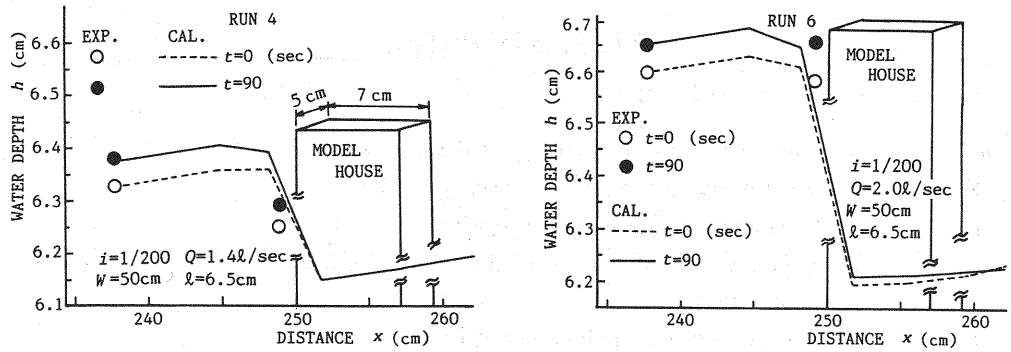

Fig.15 Comparison of the calculated and measured longitudinal water surface profiles around the model houses (total pieces of driftwood, 890)

equations of fluid motion also was refined by introducing the Adams–Bashforth scheme for time integration and the QUICK scheme for the integration of convection terms. The equation of the rotational motion of driftwood then was evaluated dynamically as was the equation of translational motion in the Lagrangian form. An interacting combination of Eulerian fluid and Lagrangian driftwood equations were used, in which the turbulent diffusivity and the fluctuation component of the rotational angular velocity of the driftwood were given stochastically. The positions and rotational angles of pieces of driftwood were well explained by the calculations. Lastly, time changes in the number of pieces of driftwood caught between and/or in front of the model houses in the experiments were well explained by the calculations. The increase in the water depth caused by the stoppage of the driftwood at the model houses also was well explained by the calculations.

The probability, $p(n)$, that driftwood coming from the rear will be stopped by n pieces of driftwood already caught between the houses, was evaluated experimentally, but as this is an important parameter that prescribes the halting rate, $\alpha(t)$, further examination is required both experimentally and mathematically.

ACKNOWLEDGMENTS

A part of this study was supported by Grant-in-Aids for General Scientific Research (B) [No.05452376] and (C) [No.05680368] from the Japanese Ministry of Education, Science and Culture. We express our gratitude to the authorities concerned.

REFERENCES

1. Hosoda. T. and I. Kimura : Vortex formation with free surface variation in shear layer of open channel flows near abrupt expansion, Proc. of Hydraulic Engg., JSCE, Vol.37, pp.463–468, 1993 (in Japanese).
2. Nakagawa, H., T. Takahashi and M. Ikeguchi : Drift wood diffusion by overland flood flow, Proc. of Hydraulic Engg., JSCE, Vol.37, pp.379–384, 1993 (in Japanese).
3. Nakagawa, H. : Behavior of overland flood flow or debris flow and its analysis, Lecture Note for the Water Engg., Committee of Hydraulics, JSCE, pp.A-9-1–A-9-20, 1992 (in Japanese).
4. Dukowicz, J.K. : A particle-fluid numerical model for liquid sprays, Jour. of Comp. Physics, Vol.35, pp.229–253, 1980.
5. Nakagawa, H., T. Takahashi and M. Ikeguchi : Driftwood behavior by overland flood flows, Jour. of Hydroscience and Hydraulic Engg., JSCE, Vol.12, No.2, pp.31–39, 1994.
6. Nakagawa, H., K. Inoue, M. Ikeguchi and T. Tsubono : Numerical simulation of driftwood behavior (2): dam up of drift wood, Annuals, Disas. Prev. Res. Inst., Kyoto Univ., No.36 B-2, pp.487–498, 1993 (in Japanese).
7. Nakagawa, H., T. Takahashi and K. Adachi : Behavior of drift wood with overland flood flow, Annuals, Disas. Prev. Res. Inst., Kyoto Univ., No.34 B-2, pp.373–386, 1991 (in Japanese).

APPENDIX–NOTATION

The following symbols are used in this paper:

a = numerical constant taking the value of 0.3;
A = small water surface area defined by $\Delta x \Delta y$;
A_h = horizontal kinematic eddy viscosity;
A_{kx}, A_{ky} = respective projected areas of the submerged part of driftwood in the x and y directions;
B = interval between the house models;
B_h = width of model house;
C_{Dx}, C_{Dy} = respective drag coefficients in the x and y directions;
C_M = virtual mass coefficient;
C_{sp} = driftwood rate supplied by the driftwood feeder per unit width and time;
f = resistance coefficient;
Fr = Froude number;
g = gravitational acceleration;
h = water depth;
H = water level;
i = channel slope;
I = moment of inertia;
k = turbulent energy;
K_x, K_y = diffusion coefficient of driftwood in the x and y directions;
ℓ = length of the piece of driftwood;
m. = fluid mass occupied by the volume of a piece of driftwood;
m_k = mass of a piece of driftwood;
M, N = respective water discharge per unit width in the x and y directions;
n = number of pieces of driftwood caught between the houses;
N_0 = moment caused by the hydrodynamic force acting on the driftwood;
N_t = number of pieces of driftwood in the area $\Delta x \Delta y$;
$p(n)$ = probability that driftwood coming from the rear will be stopped by n pieces of driftwood already caught between the houses;
q = random variable uniformly distributed in the range [0,1];
Q = water discharge;
r = radius of the driftwood;
Re = Reynolds number;
t = time;
t_{en} = time of arrival of the last piece of driftwood at the model house measured from the time of arrival of the first piece;
u, v = respective depth-averaged velocity components in the x and y directions;
u_k, v_k = respective velocity components of driftwood in the x and y directions;

u_*	=	friction velocity;
U_k, V_k	=	respective local velocity components of the fluid in the x and y directions at the centroid position of the driftwood;
W	=	channel width;
W_k	=	relative velocity of the fluid with respect to the driftwood, i.e., $W_k = \sqrt{(u_k - U_k)^2 + (v_k - V_k)^2}$;
x, y	=	coordinates of the fluid;
X, Y	=	coordinates of the driftwood position;
z_b	=	elevation of the bed;
α, β	=	random variables independently uniformly distributed in the range [0, 1];
$\alpha(t)$	=	halting rate of the driftwood at the model house;
Δt	=	time interval in the finite difference equations;
$\Delta x, \Delta y$	=	respective spatial mesh sizes in the x and y directions in the finite difference equations;
$\Delta X_k, \Delta Y_k$	=	respective fluctuation components of driftwood position in the x and y directions;
γ	=	$(\omega_p - \overline{\omega})/\sigma_\omega$;
η	=	variable of integration;
θ_k	=	rotational angle of the driftwood;
ν	=	kinematic viscosity;
ρ	=	density of the fluid;
ρ_d	=	density of the driftwood;
σ_ω	=	standard deviation of the rotational angular velocity of the driftwood;
τ_{sx}, τ_{sy}	=	respective shear stresses at the water surface in the x and y directions;
π	=	ratio of the circumference of a circle to its diameter;
Φ	=	distribution function of the probability density function;
ω	=	rotational angular velocity of the driftwood;
$\overline{\omega}$	=	mean value of the rotational angular velocity of the driftwood; and
ω_d, ω_p	=	respective deterministically and stochastically evaluated rotational angular velocity of the driftwood.